nature neuroscience

BRIEF COMMUNICATION

https://doi.org/10.1038/s41593-020-0623-9

Primate auditory prototype in the evolution of the arcuate fasciculus

Fabien Balezeau[1,8] ✉, Benjamin Wilson[1,7,8] ✉, Guillermo Gallardo[2], Fred Dick[3], William Hopkins[4], Alfred Anwander[2], Angela D. Friederici[2], Timothy D. Griffiths[1,5,6,9] and Christopher I. Petkov[1,9] ✉

The human arcuate fasciculus pathway is crucial for language, interconnecting posterior temporal and inferior frontal areas. Whether a monkey homolog exists is controversial and the nature of human-specific specialization unclear. Using monkey, ape and human auditory functional fields and diffusion-weighted MRI, we identified homologous pathways originating from the auditory cortex. This discovery establishes a primate auditory prototype for the arcuate fasciculus, reveals an earlier phylogenetic origin and illuminates its remarkable transformation.

The human arcuate fasciculus (AF) is a dorsal brain pathway critical for language[1]. It matures during childhood into a dominant and left-hemisphere lateralized pathway[2], damage to which results in language disorders[3]. Insights on AF evolution are important to understand the emergence of language and human-specific brain specialization.

Chimpanzees (an ape species) possess an AF homolog that interconnects the posterior temporal and inferior frontal areas; however, the extent to which macaques (a monkey species) have a similar pathway is controversial[4–9] (Fig. 1a). Current accounts[7,10,11] link AF evolutionary differentiation with expansion of the middle temporal gyrus (MTG), a prominent gyrus in humans that is evident in chimpanzees but not monkeys[6,7,10]. It follows that MTG projections to the inferior frontal cortex (IFC) via an AF homolog, if present in ape and human common ancestors, would not be unique to modern humans or language. Further human differentiation of MTG and AF is believed to have coincided with language evolution, but the nature and evolutionary context of human-specific AF specialization is poorly understood.

In this study, we addressed the question of whether a monkey frontotemporal homolog of the AF might exist despite the absence of an MTG in monkeys. We functionally defined the probable origin of an auditory segment of this pathway in rhesus macaques, chimpanzees and humans, using auditory tonotopic information and probabilistic diffusion-weighted MRI (dMRI) tractography. Projection patterns from the auditory cortex (AC) in monkeys, although often assumed to rely on a ventral rather than dorsal pathway, required direct comparison to other primates. It was also unclear the extent to which previous comparative neuroimaging studies compared temporal lobe areas with different functions (that is, auditory, visual or associative) across species and thus different connectivity (Fig. 1a). We demonstrated that a symmetrical auditory evolutionary prototype of the human AF originating in the AC exists in both macaques and chimpanzees and that a critical evolutionary lateralization of this pathway occurred in humans.

First, we leveraged an openly available, ultra-high resolution (200 µm) postmortem macaque dMRI dataset[12]. Exploratory analyses revealed considerable dorsal pathway connections between posterior supratemporal areas and the IFC in both hemispheres (Fig. 1b).

Next, given that humans are often studied awake during dMRI, we worked to collect original awake dMRI datasets in three macaques (5 scans, approximately 75 min per animal), informed by a functional MRI (fMRI) probabilistic tonotopic map obtained in several macaques to approximate the location of auditory cortical fields (ACFs; Methods). To determine which ACFs project to the IFC and whether by ventral or dorsal pathways, ACF regions of interest (ROIs; Fig. 1c) were used as seeds in deterministic (see Extended Data Fig. 1) and probabilistic analyses, corrected for partial volume effects and spurious dorsal pathway projections (Methods and Extended Data Fig. 2). In all three macaques, the ventral pathway was prominent from more anterior ACFs (Fig. 1d,e). However, a clear dorsal pathway to the IFC was also found, arising particularly from posteromedial ACFs (for example, middle medial (MM), primary AC (A1) and caudomedial (CM) fields). Comparing coronal sections to a standard macaque atlas on fiber pathways[13] shows that this dorsal auditory pathway involves the macaque AF homolog and portions of the superior longitudinal fasciculus II/III (Extended Data Fig. 3). We quantified effects using dorsal and ventral waypoint analyses (Fig. 1e). Testing these macaque data showed a dorsal versus ventral pathway effect (repeated measures analysis of variance (ANOVA), $p = 0.003$; Methods) but no hemisphere effect or interaction with pathway and hemisphere.

In chimpanzees, we conducted similar analyses on dMRI datasets in three animals scanned while anesthetized after a regular veterinary checkup (Methods). We used three anatomically defined auditory ROIs based on previous tonotopic results in apes[14] and the location of the chimpanzee Heschl's gyrus (AC) homolog (Fig. 2a). As in macaques, probabilistic tractography identified ventral and dorsal pathways in the chimpanzees (Fig. 2a). As with macaques,

[1]Newcastle University Medical School, Newcastle upon Tyne, UK. [2]Max Planck Institute for Cognitive and Brain Sciences, Department of Neuropsychology, Leipzig, Germany. [3]Birkbeck-UCL Centre for NeuroImaging, Birkbeck University of London, London, UK. [4]Keeling Center for Comparative Medicine and Research at University of Texas MD Anderson Cancer Center, TX, Bastrop, USA. [5]Wellcome Trust Centre for Neuroimaging, University College London, London, UK. [6]Department of Neurosurgery, University of Iowa Hospitals and Clinics, IA, Iowa City, USA. [7]Present address: Department of Psychology and Yerkes Primate Research Center, Emory University, GA, Atlanta, USA. [8]These authors contributed equally: Fabien Balezeau, Benjamin Wilson. [9] These authors jointly supervised this work: Timothy D. Griffiths, Christopher I. Petkov. ✉e-mail: fabien.balezeau@newcastle.ac.uk; benjamin.wilson@emory.edu; chris.petkov@newcastle.ac.uk

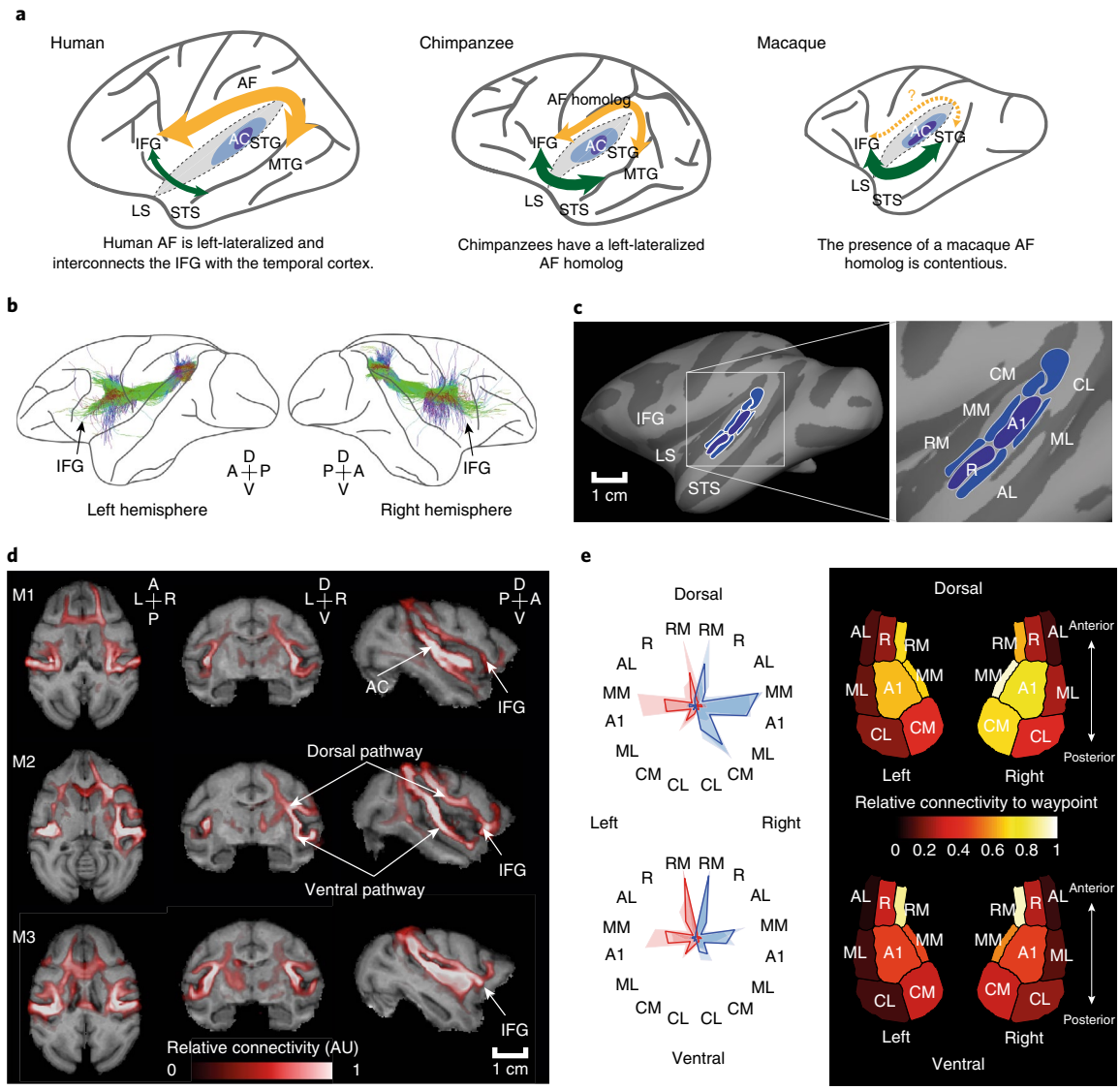

Fig. 1 | Existing view and evidence for monkey dorsal and ventral auditory pathways. a, Illustration of the existing view on AF evolution originating with a common ancestor to humans and chimpanzees[1,4–11,15,17]. The dashed lines illustrate an expanded lateral sulcus (LS) showing the location of the AC on the superior temporal plane. **b**, Deterministic tractography in the ultra-high resolution ex vivo macaque dMRI dataset[12]. Green, anteroposterior; blue, dorsoventral; red, mediolateral. **c**, fMRI tonotopically defined core (dark blue) and belt (light blue) ACFs, each based on a gradient of low- to high-frequency selectivity. **d**, Awake macaque probabilistic tractography (relative connectivity arbitrary units (AU)) showing the dorsal and ventral connections between the IFC and a posteromedial ACF (MM). **e**, Connectivity from the ACFs via dorsal and ventral pathways. Mean relative connectivity fingerprints (thick lines) and individual variability (shaded) in the left (red) and right hemisphere (blue); these are shown on a model of ACFs as heatmaps (right). See also Extended Data Fig. 4. IFG, inferior frontal gyrus.

both ventral and dorsal projections from auditory seed regions were largely symmetrical across the hemispheres (Methods). This result differs from previous evidence of ape dorsal pathway projections from broader temporal lobe sites, including association and visual cortical areas, which are left-lateralized as in humans[10].

In humans, we used ACF seeds from human tonotopic fMRI maps (Fig. 2b) to analyze three dMRI datasets. Probabilistic tractography replicated previous findings, showing more pronounced dorsal versus ventral pathways (Fig. 2c,d), and we identified an auditory segment of the human AF. In contrast to the observations in macaques and chimpanzees, the auditory segment of the human AF appears left-lateralized, particularly from posteromedial ACFs (compare with Takaya et al.[15]). We found a significantly stronger dorsal versus ventral pathway effect ($P=0.031$) and a statistical trend in the left hemisphere effect and interaction, with pathway as a factor (both $P<0.06$; Methods).

Finally, we quantified and compared the connectivity of the AC projections from both pathways in all three species. In line with previous findings, the ventral pathway was predominant in macaques and chimpanzees, with the dorsal pathway predominating in humans (a cross-species repeated measures ANOVA showed a species and pathway interaction, $P=0.003$). We also observed a significant interaction of species, pathway and hemisphere ($P=0.002$) driven by the left-lateralized human AC dorsal pathway (Fig. 3) relative to the more symmetrical pattern in apes and monkeys.

This work provides new insights into the evolutionary origins of the AF. It establishes an auditory segment of the human AF and provides evidence for homologous pathways in chimpanzees and

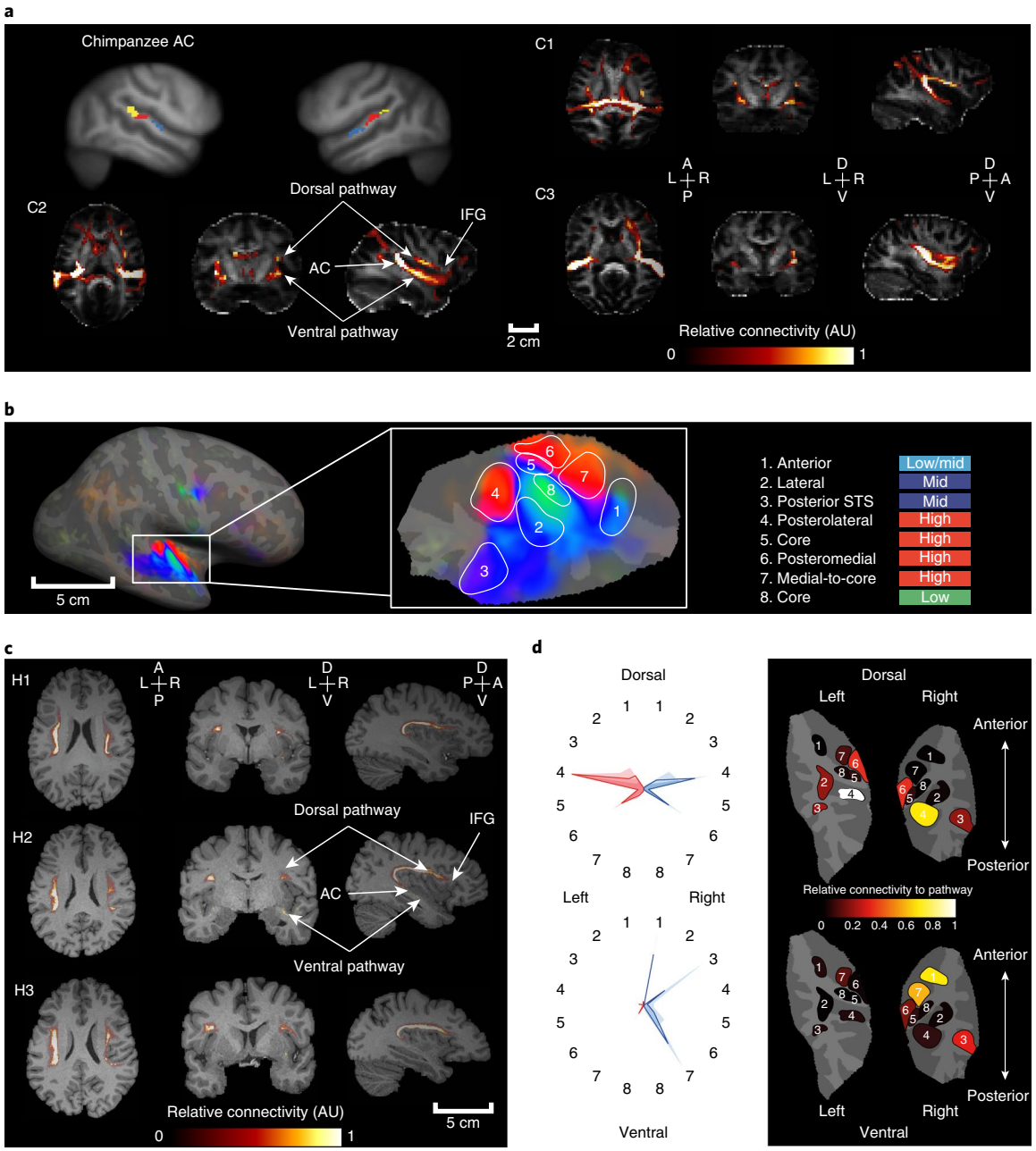

Fig. 2 | Chimpanzee and human tractography of auditory dorsal and ventral pathways. a, Chimpanzee probabilistic tractography between the auditory seed regions and the IFC. **b**, Tonotopically defined human ACFs: regions 5 and 8 together may constitute a primary 'core' ACF; the surrounding frequency selective areas (1–4, 6 and 7) capture at least parts of the adjacent ACFs (Methods). **c**, Human probabilistic tractography between the auditory seed regions and the IFC. **d**, Human connectivity from ACFs via the dorsal and ventral pathways. Mean relative connectivity fingerprints (thick lines) and individual variability (shaded) in the left (red) and right hemispheres (blue); these are shown on ACFs as heatmaps (right).

macaques. The auditory dorsal pathway's lack of strong asymmetry in nonhuman primates is in stark contrast to the left-hemisphere asymmetry seen in humans in this study and elsewhere[15]. The findings advance an intriguing explanatory account of human AF evolution, addressing (1) the evolutionarily conserved primate prototype, (2) when it may have emerged and (3) human-specific differentiation.

Current accounts of human AF evolution[7,10,11] are based on evolutionary changes predating human language evolution, thought to have begun to take form in ape and human ancestors (Fig. 1a). A key evolutionary change is often linked to the presence of the MTG in apes and the further expansion of AF connectivity from it in human ancestors[7]. This account often assumes a greater visual role of the macaque dorsal pathways, for example, monkey dorsal pathway projections from the parietal cortex[11]. Given that chimpanzee dMRI had previously shown left-hemisphere asymmetry in the dorsal pathway from other temporal lobe areas[10], it could previously be assumed that all the pieces began to take form in ancestors to apes and humans, followed by further differentiation in human ancestors.

The current results advance a primate auditory prototype hypothesis, raising the possibility that our shared ancestors with apes and monkeys possessed symmetrical dorsal pathways interconnecting auditory temporal lobe regions with the IFC (Fig. 3). The left-hemisphere auditory AF connectivity pattern in humans

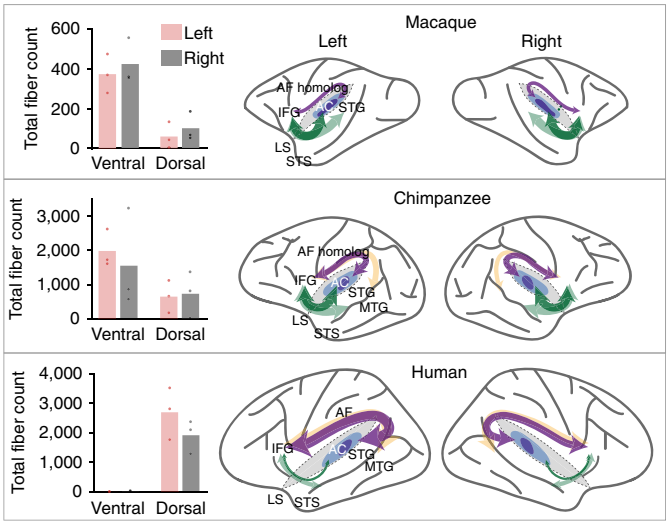

Fig. 3 | Summary of auditory dorsal and ventral pathway strength and lateralization in macaques, chimpanzees and humans. Left: bar plots showing the individual results and mean fiber counts for the left and right dorsal and ventral pathways for each of the three species. Right: schematic summary of the dorsal (purple) and ventral (dark green) pathway results in macaques, chimpanzees and humans, overlaid on previous observations (light yellow and light green). Our results replicate key observations from previous studies using other or broader temporal lobe seeds as follows: stronger dorsal than ventral pathway in humans[2,8,10], stronger ventral than dorsal pathway in chimpanzees[10], a prominent ventral pathway in macaques[7] and a symmetrical ventral pathway (green) in all three species[7,10]. The insights into AF evolution stemming from using the functionally defined seeds are as follows: homologous ventral (dark green) and dorsal (purple) pathways from the AC in all three species, with the AF segment left-lateralized in humans but not so lateralized in nonhuman primates. These findings support the primate auditory prototype hypothesis.

appears to have differentiated further from this primate auditory prototype. The hypothesis also posits a key point of differentiation that appears to have occurred uniquely in the human lineage: the differentiation of the human right dorsal pathway connectivity away from the auditory prototype to involve more caudal temporal and parietal areas[15].

The contribution to the dorsal pathway from auditory areas is interesting and perhaps surprising, in that an evolutionarily conserved system relies on relatively early-stage auditory cortical input via ventral and dorsal pathways. In macaques, anterograde tractography has shown that the prefrontal cortex receives monosynaptic auditory input from the belt AC[16]. Our dMRI observations across species have identified the auditory segment of the dorsal pathway and pushed back the emergence of the auditory prototype of the AF further than the split from a common ancestor with macaques (approximately 25 million years ago), rather than the 5 million years ago previously assumed, when humans and chimpanzees last shared a common ancestor.

Our observations fit with the notion that language adaptations may have arisen from primate auditory pathways[17]. We speculate that this dorsal auditory pathway is involved in not just spatial processing in the classical sense but also sound and vocal patterning in the time domain[18], which is supported by evidence implicating the IFC in sound sequence patterning in macaques and humans[19] and vocalization sound processing and production in macaques, marmosets and humans[20]. Whereas auditory processes in monkeys may have previously been assumed to involve ventral pathways, the current results indicate that a dorsal auditory pathway in macaques should not be dismissed. Future studies could assess the extent to which New World monkeys, prosimians or even nonprimate species might have an auditory dorsal pathway to the IFC, to pinpoint its earliest evolutionary origin.

Online content

Any methods, additional references, Nature Research reporting summaries, source data, extended data, supplementary information, acknowledgements, peer review information; details of author contributions and competing interests; and statements of data and code availability are available at https://doi.org/10.1038/s41593-020-0623-9.

Received: 15 November 2019; Accepted: 16 March 2020;
Published online: 20 April 2020

References

1. Hagoort, P. The neurobiology of language beyond single-word processing. *Science* **366**, 55–58 (2019).
2. Anwander, A., Tittgemeyer, M., von Cramon, D. Y., Friederici, A. D. & Knösche, T. R. Connectivity-based parcellation of Broca's area. *Cereb. Cortex* **17**, 816–825 (2007).
3. Price, C. J., Seghier, M. L. & Leff, A. P. Predicting language outcome and recovery after stroke: the PLORAS system. *Nat. Rev. Neurol.* **6**, 202–210 (2010).
4. Bornkessel-Schlesewsky, I., Schlesewsky, M., Small, S. L. & Rauschecker, J. P. Neurobiological roots of language in primate audition: common computational properties.*Trends Cogn. Sci.* **19**, 142–150 (2015).
5. Skeide, M. A. & Friederici, A. D. Response to Bornkessel-Schlesewsky *et al.*—Towards a nonhuman primate model of language? *Trends Cogn. Sci.* **19**, 483 (2015).
6. Thiebaut de Schotten, M., Dell'Acqua, F., Valabregue, R. & Catani, M. Monkey to human comparative anatomy of the frontal lobe association tracts. *Cortex* **48**, 82–96 (2012).
7. Rilling, J. K. et al. The evolution of the arcuate fasciculus revealed with comparative DTI. *Nat. Neurosci.* **11**, 426–428 (2008).
8. Eichert, N. et al. What is special about the human arcuate fasciculus? Lateralization, projections, and expansion. *Cortex* **118**, 107–115 (2019).
9. Frey, S., Mackey, S. & Petrides, M. Cortico-cortical connections of areas 44 and 45B in the macaque monkey. *Brain Lang.* **131**, 36–55 (2014).
10. Rilling, J., Glasser, M. F., Jbabdi, S., Andersson, J. & Preuss, T. M. Continuity, divergence, and the evolution of brain language pathways. *Front. Evol. Neurosci.* **3**, 11 (2012).
11. Mars, R. B., Eichert, N., Jbabdi, S., Verhagen, L. & Rushworth, M. F. S. Connectivity and the search for specializations in the language-capable brain. *Curr. Opin. Behav. Sci.* **21**, 19–26 (2018).
12. Calabrese, E. et al. A diffusion tensor MRI atlas of the postmortem rhesus macaque Brain. *Neuroimage* **117**, 408–416 (2015).
13. Schmahmann J. D. & Pandya D. N. *Fiber Pathways of the Brain* (Oxford Univ. Press, 2009).
14. Bailey, P., Von Bonin, G., Garol, H. W. & McCulloch, W. S. Functional organization of temporal lobe of monkey (*Macaca mulatta*) and chimpanzee (*Pan satyrus*). *J. Neurophysiol.* **6**, 121–128 (1943).
15. Takaya, S. et al. Asymmetric projections of the arcuate fasciculus to the temporal cortex underlie lateralized language function in the human brain. *Front. Neuroanat.* **9**, 119 (2015).
16. Romanski, L. M. et al. Dual streams of auditory afferents target multiple domains in the primate prefrontal cortex. *Nat. Neurosci.* **2**, 1131–1136 (1999).
17. Rauschecker, J. P. & Scott, S. K. Maps and streams in the auditory cortex: nonhuman primates illuminate human speech processing. *Nat. Neurosci.* **12**, 718–724 (2009).
18. Zhang, Y. S. & Ghazanfar, A. A. A hierarchy of autonomous systems for vocal production. *Trends Neurosci.* **43**, P115–P126 (2020).
19. Wilson, B. et al. Auditory sequence processing reveals evolutionarily conserved regions of frontal cortex in macaques and humans. *Nat. Commun.* **6**, 8901 (2015).
20. Flinker, A. & Knight, R. T. Broca's area in comprehension and production, insights from intracranial studies in humans. *Curr. Opin. Behav. Sci.* **21**, 170–175 (2018).

Methods

Overview of dMRI datasets. The postmortem macaque ultra-high resolution dMRI dataset was obtained via an openly shared resource[12]. The dMRI datasets in the three awake male macaques were obtained as described in the following sections, with a probabilistic fMRI tonotopic map based on Petkov et al.[21] and Baumann et al.[22]. The dMRI scans of three anesthetized male chimpanzees were obtained via the National Chimpanzee Brain Resource (http://www.chimpanzeebrain.org), with AC location as detailed in the following sections. The awake adult human diffusion datasets were obtained from an openly shared resource[23], with an fMRI tonotopic map based on Dick et al.[24].

Macaque awake datasets. dMRI scans were acquired in three adult male rhesus macaques (*Macaca mulatta*): M1, M2 and M3 weighing 10, 16 and 12 kg, respectively and aged 10, 13 and 7. The three macaques were visually assessed for their preferred hand when grasping objects (for example, food): M1 and M3 were mostly bimanual, showing no preference for hand of use, and M2 showed right hand preference. There was no obvious relationship with handedness in the macaque results.

All procedures conducted with the macaques were approved by the Animal Welfare and Ethical Review Body and the UK Home Office and are in full compliance with both the UK Animal Scientific Procedures Act and the European Directive 2010/63/EU on the care and use of animals in research. We support the guidelines of the consortium on Animal Research: Reporting of In Vivo Experiments. Given the ethical sensitivities involved in research with nonhuman primates and the 3Rs principles (one of which is on the reduction of animal numbers), our work with awake macaques required using the fewest animals necessary. A sample size of 2–3 is common in behavioral neuroscience experiments with macaques, provided that results are robust within each individual and that the effects generalize beyond one animal, as indeed they do (see main text). Training macaques for awake MRI requires a substantial time investment; the data that were combined for each of these datasets in each of the three animals are robust and consistent across the three animals. The same sample size in chimpanzees and humans allowed cross-species comparisons. Thus, there was little ethical justification to train and test additional monkeys.

Awake macaque dMRI procedure. Macaques were scanned sitting in a primate chair within a vertical MRI scanner (Biospec 4.7 Tesla; Bruker). The macaques had all been previously acclimatized to the scanner environment and to the length of scanning required; they were trained for an fMRI scanning task, including periodic fixation under head immobilization, using operant training[19]. Macaques were rewarded with juice for fixating a central spot on the screen for 2–4 s, as measured with an infrared eye tracker (ISCAN).

A four-channel receiver surface coil array and a saddle transmitter coil were used for MRI acquisition (Windmiller Kolster Scientific). The sequence used was diffusion-weighted spin-echo echo-planar imaging with the following parameters: echo time = 58 ms; repetition time = 14,200 ms; matrix 88 × 88; 56 slices; for a voxel size of 0.97 × 0.97 × 1 mm^3. Twofold generalized autocalibrating partial parallel acquisition acceleration was applied to obtain low distortion, high resolution and motion-robust acquisition. B_0 field uniformity was optimized using the MAPSHIM algorithm along first- and second-order shim gradients (Bruker). To provide the best possible fiber discrimination and tracking, we used a high angular resolution diffusion imaging approach with the highest spatial resolution enabled by the hardware at 4.7 T. We acquired 60 diffusions directions ($b = 850\ s\ mm^{-2}$) and four $b = 0$ images. The scan was repeated five times to improve the signal-to-noise ratio. Total scan duration was approximately 75 min for each animal. Saturation slices were used to suppress the signal from the temporal muscles, eyes and mouth. This also enabled us to reduce the field of view and thus increase the scanning resolution. A fat suppression preparation pulse was applied to reduce ghosting artifacts.

Awake macaque diffusion data processing. Deterministic dMRI was performed using the BioImage Suite (v3.01; Yale School of Medicine). Deterministic tracking (see Extended Data Fig. 1) was used primarily for visualization purposes since the result will always follow the largest dominant fractional anisotropy values. However, deterministic tracking has a high false negative rate and there was no clear evidence in any but one of the animals of a dorsal pathway with this approach (Extended Data Fig. 1). Two ventral pathways were consistently observed in every animal, medially (extreme capsule and uncinate fasciculus pathways) and laterally (middle longitudinal fasciculus) interconnecting the anterior ACFs with other temporal lobe sites and the IFC. Cross-callosal connections and those to the parietal cortex, auditory thalamus (medial geniculate nucleus) and inferior colliculus were also observed using this approach in most animals.

The FSL Toolbox[25] FDT tool v.6.0.1 was used to compute a more complex diffusion model and perform probabilistic fiber tracking[26]. Diffusion parameters were computed using Bayesian estimation of diffusion parameters obtained using sampling techniques with crossing fibers (BEDPOSTX) with default settings (two fibers, weight 1). Fiber tracking was performed by probabilistic tracking with crossing fibers (PROBTRACKX) using default setting (5,000 samples, curvature threshold = 0.2), with a given ROI mask as the seed region. Probabilistic tracking for a given seed voxel or region provides a connectivity index map in the form of a streamline (fiber) count for each voxel.

Seed regions for fiber tracking were defined based on ACF tonotopic mapping along the superior temporal plane[21,22]. ACF ROIs included the auditory core (A1, rostral (R), rostrotemporal (RT)) and belt areas (caudolateral (CL), CM, mediolateral (ML), MM, anterolateral (AL), anteromedial (AM), lateral rostrotemporal (RTL), medial rostrotemporal (RTM)) drawn from a volumetric probabilistic tonotopic map defined from majority overlap in ACF locations in a coregistered group of ten macaques scanned awake over the last ten years. The probabilistic map was registered to the individual native-space dMRI fractional anisotropy maps for each animal.

All ROI voxels were inspected for partial volume effects and anatomical structure misregistration, correcting, if needed, the ROI overlap or anatomical involvement of nonauditory regions before further analysis. We excluded voxels in the superior temporal sulcus (STS) or the dorsal bank of the lateral sulcus (LS). The ACF ROIs were also restricted to gray matter using FSL's FAST white matter segmentation tool as a white matter exclusion mask[27]. To avoid artifactual dorsal pathway voxels not emanating from the AC, a volumetric exclusion mask was defined covering the full extent of the sylvian fissure (LS) separating the superior temporal plane and dorsal regions in the frontal and parietal cortex (Extended Data Fig. 2). Omission of this mask causes strong false positive dorsal pathway involvement because some AC voxels in the superior temporal plane are mislocalized to the dorsal LS owing to partial volume effects. The LS exclusion mask ensures that the analyses are more conservative with regard to spurious dorsal supratemporal plane to IFC pathway connectivity.

Dorsal and ventral waypoints were defined as ROIs to compare the relative strength of the pathways based on the probabilistic tracking results in each animal (Fig. 1d). For each functionally defined seed ACF region (for example, A1, CM, etc.), the mean connectivity index value was extracted from the voxels in these anatomically defined ROIs. Connectivity measurements (fiber count) are shown and were used for further analysis as indicated. Figure 1c,e does not show the more rostral ACFs (RTM, RT and RTL) because these regions do not show dorsal pathway projections. Figure 1e shows the normalized connectivity from each ACF via the dorsal and ventral pathways, in each hemisphere. Macaque 3 had low signal-to-noise ratio in one hemisphere that may be implant-related and could not be avoided, affecting the dorsal pathway in the left hemisphere. Therefore, to avoid suggesting spurious right lateralization effects, these data were omitted from the illustrative heatmap summary in Fig. 1e but are included in the other analyses. The connectivity results are displayed on a model of ACFs (Fig. 1e) and rendered on the cortical surface (Extended Data Fig. 4).

Statistics. We used repeated measures ANOVA models to test the relative connectivity between inferior frontal cortex and AC in the left and right hemispheres: within-participant factors of pathway (dorsal, ventral) and hemisphere (left, right). The results for the macaque model ($n = 3$ animals) showed a main effect of pathway ($F_{1,2} = 211.4$, $P = 0.005$), indicating a stronger ventral than dorsal pathway, but no main effect of hemisphere ($F_{1,2} = 4.06$, $P = 0.181$) or interaction ($F_{1,2} = 0.294$, $P = 0.642$). The data and variance distributions of this model fitted the assumptions of the analysis. No statistical methods were used to predetermine sample sizes but our sample sizes are similar to those used previously[6–9,12,13,16,19]. Data collection could not be blinded to species or individuals, but the analyses used predefined seed regions and waypoint crossings and were conducted in the same way, that is, agnostic to the conditions being analyzed.

Chimpanzee dMRI analyses. The chimpanzee datasets were provided already preprocessed using FSL BEDPOSTX (http://www.chimpanzeebrain.org). The three male chimpanzees (aged 15, 20 and 21 years) had been visually assessed for their hand of preference. C1 and C2 preferred using the right hand. C3 preferred using the left hand. There was no obvious relationship with handedness in the chimpanzee results.

Fiber tracking was performed with PROBTRACKX using default settings, with a given auditory ROI mask as the seed region. Three auditory cortical areas were defined by placing ROIs over the chimpanzee transverse temporal gyrus, the center of the presumed homolog of the human Heschl's gyrus[12,28], and two regions either posterior or anterior to it of similar size, all restricted to gray matter (Fig. 2a). Unlike the macaques, an LS exclusion mask was not necessary given the larger ape brain and the greater separation of dorsal and ventral banks of the LS, naturally reducing partial volume effects. The volumetric ROIs were restricted to the gray matter and distanced from the LS by at least a voxel to prevent tracking via nonauditory regions dorsal to AC.

Statistics. Statistical testing of the dorsal versus ventral and left versus right fiber counts across the three chimpanzees used a repeated measures ANOVA: within-participant factors of pathway (dorsal, ventral) and hemisphere (left, right). The data and variance distributions fitted the assumptions of the analysis. In the chimpanzee model ($n = 3$ animals), we observed no significant effects of pathway ($F_{1,2} = 3.33$, $P = 0.209$), hemisphere ($F_{1,2} = 0.104$, $P = 0.778$) or higher-order interactions between these factors ($F_{1,2} = 11.773$, $P = 0.075$). No statistical methods were used to predetermine sample sizes but our sample sizes are similar to those

used previously[7,14,28]. Data collection could not be blinded to species or individuals, but the analyses used predefined seed regions and waypoint crossings and were conducted in the same way, that is, agnostic to the conditions being analyzed.

Human dMRI analyses. Three male individuals between 25 and 32 years old were randomly selected from the S500 group of the Human Connectome Project. All three individuals had already been preprocessed with the Human Connectome Project minimum pipeline. Auditory ROIs were based on a combination of frequency band activity preferences and estimated myelin map discontinuities ($n=55$) in cross-individual, surface-based averages defined on the cortical surface of an individual whose brain had been morphed to the MNI atlas before surface reconstruction in FreeSurfer (v5.3.0 and csurf v0.8). ACF ROIs are shown in Fig. 2b, overlaid on the average tonotopic map of the right hemisphere. The two 'auditory core' ROIs (ACF numbers 5 and 8 in Fig. 2c) were defined within a patch of maximal R1 intensity and delineated by higher- and lower-frequency preferences. The other 'belt/parabelt' ROIs were defined from the medial and lateral borders of the anterior auditory core: the anterior ROI (1 in Fig. 2b) was more weakly tonotopic on average and it straddled a low- to medium-frequency preference region. The more lateral ROI was a patch with lower-frequency preference along the superior temporal gyrus (STG) (2 in Fig. 2b), and the more medial one was within a higher-frequency preference region (7 in Fig. 2b). The posterior belt/parabelt ROIs (6 and 4 in Fig. 2b) straddled the posterior aspect of the core field (5 and 8) and showed high-frequency preference. The posterolateral ROI (3 in Fig. 2b) encompassed a tonotopic region with middle-frequency preference lateral to the R1 hyperintense band notable along the STG.

Each ROI was surface-morphed from the individual to FreeSurfer's fsaverage and was then projected into the cortex (from 10% below the white/gray border to the pial surface) of the 2-mm isotropic resolution MNI-152 volume. The three human participants were registered to the MNI space using a nonlinear registration algorithm (FSL's FLIRT and FNIRT). Then, the inverse transform was applied to each volumetric ROI to bring them into each participant's space. To estimate the connectivity of each ROI to the IFC, volumetric probabilistic tractography was performed using the constrained spherical deconvolution[29] implementation on MRtrix (v3.0 RC3-137, built using Eigen 3.3.7; 1,000 streamlines option).

Statistics. As in the macaques and chimpanzees, we conducted a repeated measures ANOVA with the within-participant factors of hemisphere (left and right) and pathway (dorsal and ventral). The data and variance distributions fitted the assumptions of the analysis. In humans ($n=3$), we observed a main effect of pathway ($F_{1,2}=30.6$, $P=0.031$), with the dorsal pathway stronger than the ventral. There was also a left-hemisphere trend for hemisphere ($F_{1,2}=15.8$, $P=0.058$) and hemisphere and pathway ($F_{1,2}=15.7$, $P=0.058$). No statistical methods were used to predetermine sample sizes but were selected to match the numbers available in macaques and chimpanzees. Data collection could not be blinded to species or individuals, but the analyses used predefined seed regions and waypoint crossings and were conducted in the same way, that is, agnostic to the conditions being analyzed.

Cross-species statistical comparisons. A repeated measures ANOVA model was implemented with all the dMRI data for the three-way cross-species comparison with the following factors: within-participant factors of pathway (dorsal, ventral), hemisphere (left, right); between individual factor of species (macaque, chimpanzee, human). The analysis showed an interaction of species and pathway ($F_{2,6}=18.1$, $P=0.003$), reflecting the relatively larger dorsal pathway in humans and ventral pathways in monkeys and apes (see Fig. 3). There was also an interaction of species, pathway and hemisphere ($F_{2,6}=20.7$, $P=0.002$) driven by the left lateralization of the human dorsal pathway relative to the more symmetrical pathways in the other two species. No other effects or interactions were significant.

Reporting Summary. Further information on research design is available in the Nature Research Reporting Summary linked to this article.

Data availability

The ultra-high resolution postmortem macaque dataset is from a previously shared resource. The chimpanzee and human datasets are from available resources (S500 group of the Human Connectome Project, http://www.chimpanzeebrain.org; the chimpanzee resource is available upon request and the NCBR staff are contacted via the main landing page). The awake macaque dMRI data is available from the Open Science Framework at https://osf.io/arqp8/ and will be made available at the PRIMatE MRI Data Exchange (https://fcon_1000.projects.nitrc.org/indi/indiPRIME.html). The ROIs are found in available atlases or as part of previous publications.

Code availability

Custom code and analyses were not required. Analysis pipelines used FSL (FDT v.6.0.1); other processing pipelines are as noted.

References

21. Petkov, C. I., Kayser, C., Augath, M. & Logothetis, N. K. Functional imaging reveals numerous fields in the monkey auditory cortex. *PLoS Biol.* **4**, e215 (2006).
22. Baumann, S. et al. Characterisation of the BOLD response time course at different levels of the auditory pathway in non-human primates. *Neuroimage* **50**, 1099–1108 (2010).
23. van Essen, D. C. et al. The Human Connectome Project: a data acquisition perspective. *Neuroimage* **62**, 2222–2231 (2012).
24. Dick, F. et al. In vivo functional and myeloarchitectonic mapping of human primary auditory areas. *J. Neurosci.* **32**, 16095–16105 (2012).
25. Smith, S. M. et al. Advances in functional and structural MR image analysis and implementation as FSL. *Neuroimage* **23**, S208–S219 (2004).
26. Behrens, T. E. J. et al. Characterization and propagation of uncertainty in diffusion-weighted MR imaging. *Magn. Reson. Med.* **50**, 1077–1088 (2003).
27. Zhang, Y., Brady, M. & Smith, S. Segmentation of brain MR images through a hidden Markov random field model and the expectation-maximization algorithm. *IEEE Trans. Med. Imaging* **20**, 45–57 (2001).
28. Hackett, T. A., Preuss, T. M. & Kaas, J. H. Architectonic identification of the core region in auditory cortex of macaques, chimpanzees, and humans. *J. Comp. Neurol.* **441**, 197–222 (2001).
29. Tournier, J.-D., Calamante, F. & Connelly, A. Robust determination of the fibre orientation distribution in diffusion MRI: non-negativity constrained super-resolved spherical deconvolution. *Neuroimage* **35**, 1459–1472 (2007).

Acknowledgements

We thank N. Eichert, R. Mars, A. Mitchell and M. Rushworth for their excellent discussion. This study was supported by the Wellcome Trust (grant no. WT091681MA to T.D.G., grant no. WT092606AIA to C.I.P. and grant no. WT110198 to B.W.); the Max Planck Society (to A.D.F. and A.A.); the European Research Council (MECHIDENT to C.I.P.); and the National Institutes of Health (Matthew Howard III with T.D.G. and C.I.P., grant no. R01-DC04290).

Author contributions

C.I.P., F.B., A.D.F. and T.D.G. conceived the study. F.B., B.W., G.G., F.D., A.A. and C.I.P. conducted the study and the analyses. F.B., B.W., G.G., F.D., W.H., A.A., A.D.F., T.D.G. and C.I.P. provided the materials. C.I.P., F.B. and B.W. wrote the paper with revisions from coauthors G.G., F.D., W.H., A.A., A.D.F. and T.D.G.

Competing interests

The authors declare no competing interests.

Additional information

Extended data is available for this paper at https://doi.org/10.1038/s41593-020-0623-9.

Supplementary information is available for this paper at https://doi.org/10.1038/s41593-020-0623-9.

Correspondence and requests for materials should be addressed to F.B., B.W. or C.I.P.

Peer review information *Nature Neuroscience* thanks Afonso Silva and the other, anonymous, reviewer(s) for their contribution to the peer review of this work.

Reprints and permissions information is available at www.nature.com/reprints.

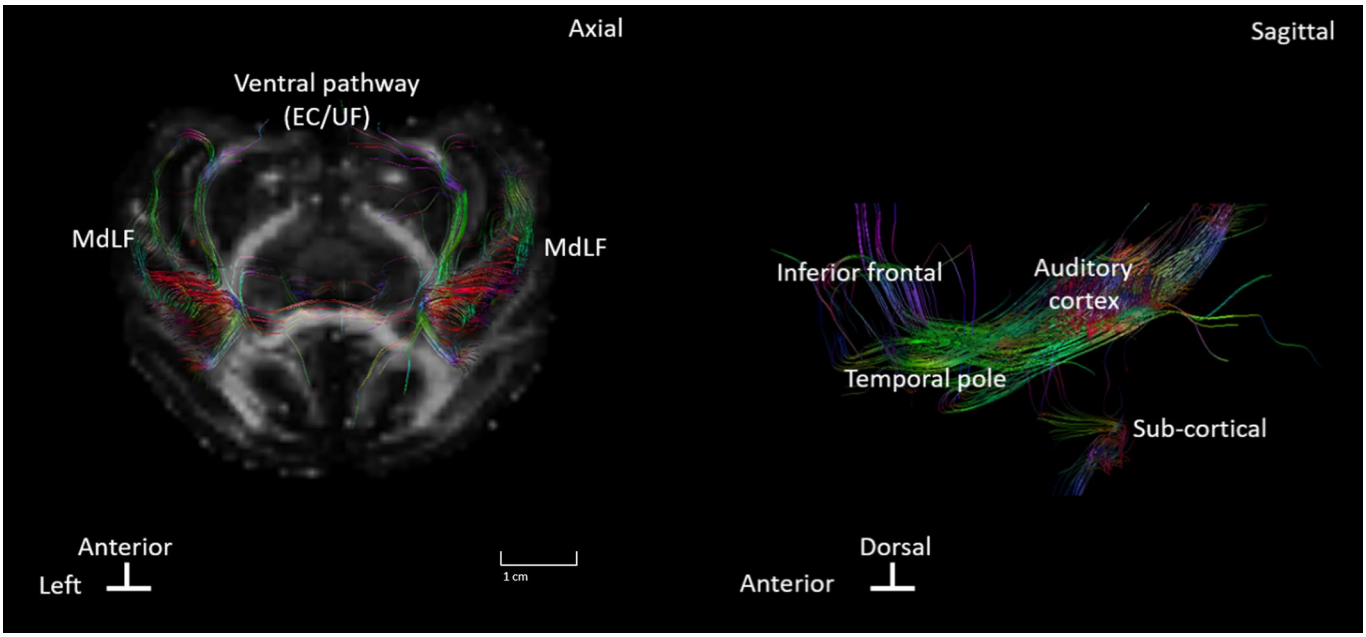

Extended Data Fig. 1 | Macaque deterministic tractography. Axial (left) and sagittal (right) slices showing diffusion weighted fractional anisotropy (FA) map overlaid with deterministic tractography. The sagittal slice shows the auditory pathways coursing to inferior frontal cortex via a ventral pathway medially involving the Uncinate Fasciculus/Extreme Capsule (UF/EC) pathway and laterally via the Middle Longitudinal Fasciculus (MdLF). No clear dorsal pathway from auditory cortex is observed using deterministic tractography. Diffusion directions, green: anterior-posterior; blue: dorsal-ventral; red: medial-lateral.

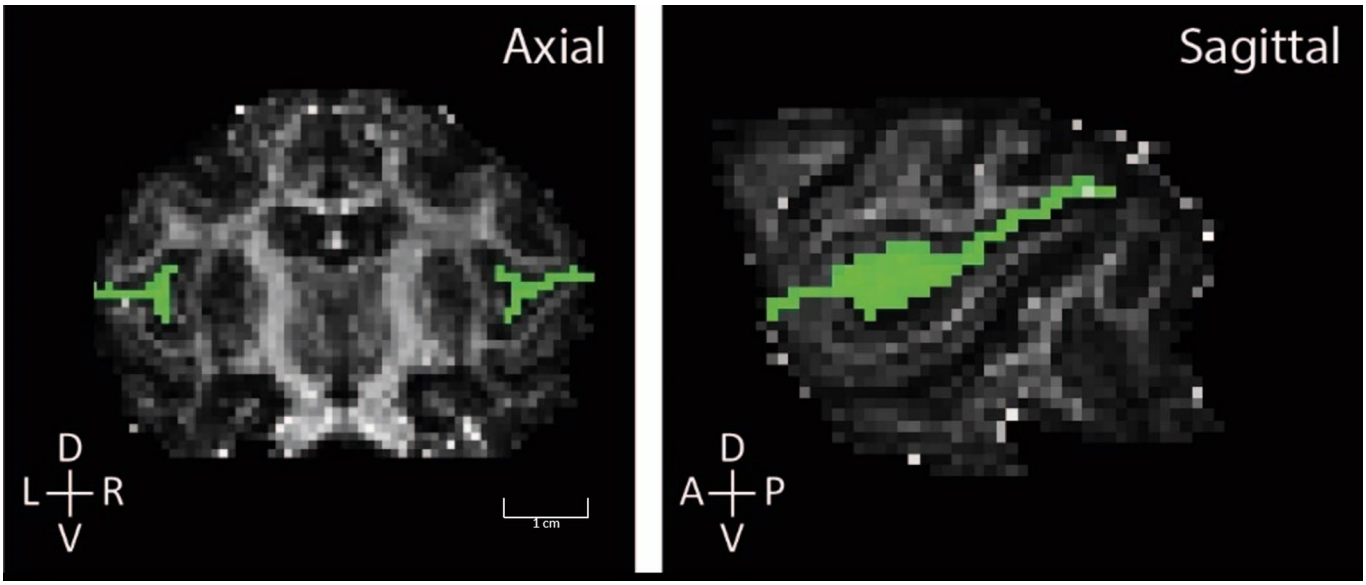

Extended Data Fig. 2 | Lateral sulcus exclusion mask in the macaques. To avoid artefactual dorsal pathway voxels not emanating from auditory cortex, an exclusion mask covering the full extent of the Sylvian fissure (lateral sulcus) separating the superior temporal plane and dorsal regions in frontal and parietal cortex was defined. Omission of this mask causes strong false positive dorsal pathways involvement because some auditory cortex voxels in the superior temporal plane are mislocalized to the dorsal lateral sulcus owing to partial volume effects. The lateral sulcus exclusion mask ensured that the analyses are more conservative with regards to spurious dorsal supra-temporal plane to inferior frontal cortex pathway connectivity.

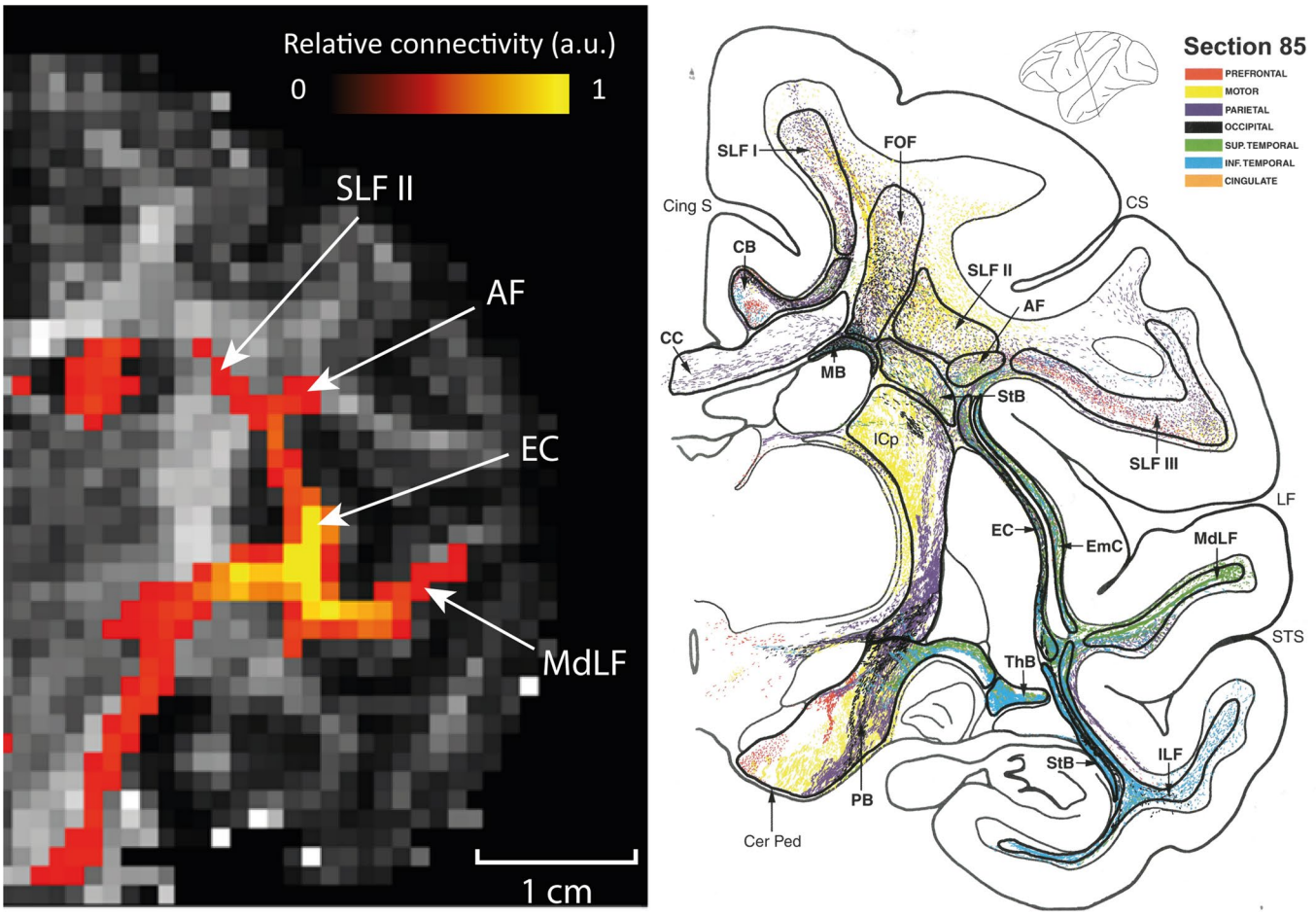

Extended Data Fig. 3 | Example comparison of probabilistic dMRI to a macaque fibre pathways atlas coronal section. Comparison of one of the coronal slices (left) showing tractography from the MM seed region, with a similarly located coronal section (right) from the Schmahmann and Pandya macaque brain pathways atlas[13] (copyright permission obtained from Oxford Publishing Limited), suggests that the dorsal pathways that we observed involve the macaque AF and parts of the Superior Longitudinal Fasciculus (SLF). SLF II/III: Superior Longitudinal Fasciculus II/III; AF: Arcuate Fasciculus; EC: Extreme Capsule pathway (Uncinate Fasciculus is visible on more anterior coronal sections); MdLF: Middle Longitudinal Fasciculus.

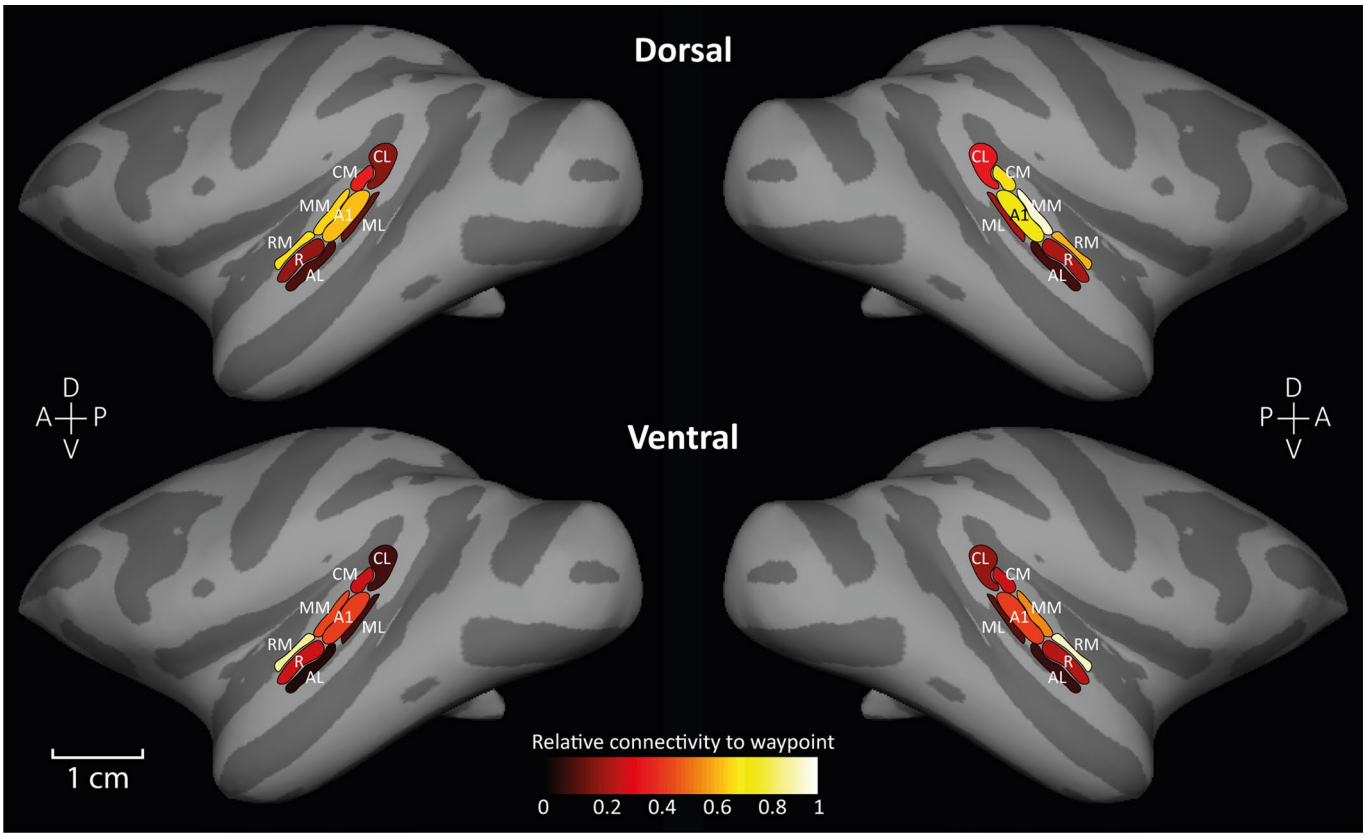

Extended Data Fig. 4 | Mean relative connectivity heat maps for each macaque auditory cortical field. Showing mean relative dorsal and ventral connectivity from each ACF (from Fig. 1e) rendered on the cortical surface for closer comparison with the human results (Fig. 2e).

nature research

Corresponding author(s): DBPR: NN-BC69971A

Last updated by author(s): 09/03/2020

Reporting Summary

Nature Research wishes to improve the reproducibility of the work that we publish. This form provides structure for consistency and transparency in reporting. For further information on Nature Research policies, see Authors & Referees and the Editorial Policy Checklist.

Statistics

For all statistical analyses, confirm that the following items are present in the figure legend, table legend, main text, or Methods section.

n/a	Confirmed	
☐	☒	The exact sample size (*n*) for each experimental group/condition, given as a discrete number and unit of measurement
☒	☐	A statement on whether measurements were taken from distinct samples or whether the same sample was measured repeatedly
☐	☒	The statistical test(s) used AND whether they are one- or two-sided *Only common tests should be described solely by name; describe more complex techniques in the Methods section.*
☒	☐	A description of all covariates tested
☐	☒	A description of any assumptions or corrections, such as tests of normality and adjustment for multiple comparisons
☒	☐	A full description of the statistical parameters including central tendency (e.g. means) or other basic estimates (e.g. regression coefficient) AND variation (e.g. standard deviation) or associated estimates of uncertainty (e.g. confidence intervals)
☐	☒	For null hypothesis testing, the test statistic (e.g. *F*, *t*, *r*) with confidence intervals, effect sizes, degrees of freedom and *P* value noted *Give P values as exact values whenever suitable.*
☒	☐	For Bayesian analysis, information on the choice of priors and Markov chain Monte Carlo settings
☒	☐	For hierarchical and complex designs, identification of the appropriate level for tests and full reporting of outcomes
☒	☐	Estimates of effect sizes (e.g. Cohen's *d*, Pearson's *r*), indicating how they were calculated

Our web collection on statistics for biologists contains articles on many of the points above.

Software and code

Policy information about availability of computer code

Data collection	Custom code or algorithms were not required. Available dMRI analyses and pipelines used the FSL software (FDT v. 6.0.1).
Data analysis	Accepted dMRI analyses pipelines were used to determine connectivity counts and analysis pipelines used FSL software (FDT v. 6.0.1).

For manuscripts utilizing custom algorithms or software that are central to the research but not yet described in published literature, software must be made available to editors/reviewers. We strongly encourage code deposition in a community repository (e.g. GitHub). See the Nature Research guidelines for submitting code & software for further information.

Data

Policy information about availability of data

All manuscripts must include a data availability statement. This statement should provide the following information, where applicable:

- Accession codes, unique identifiers, or web links for publicly available datasets
- A list of figures that have associated raw data
- A description of any restrictions on data availability

Data availability statement: The ultra-high resolution post mortem macaque dataset is from a previously shared resource. The chimpanzee and human datasets are from available resources (http://www.chimpanzeebrain.org, group S500 of the Human Connectome Project). The awake macaque dMRI data is available from Open Science Framework, accessing code (https://osf.io/arqp8/) and will be made available in the primate MRI open data sharing resource (PRIME-DE: http://fcon_1000.projects.nitrc.org/indi/indiPRIME.html). The regions of interest are available in available atlases or as part of prior publications.

Field-specific reporting

Please select the one below that is the best fit for your research. If you are not sure, read the appropriate sections before making your selection.

☒ Life sciences ☐ Behavioural & social sciences ☐ Ecological, evolutionary & environmental sciences

For a reference copy of the document with all sections, see nature.com/documents/nr-reporting-summary-flat.pdf

Life sciences study design

All studies must disclose on these points even when the disclosure is negative.

Sample size	Diffusion-weighted MRI scans were acquired in three adult male rhesus macaques (macaca mulatta). Given the ethical sensitivities involved in research with nonhuman primates and the 3Rs principles (one of which is on the Reduction of animal numbers), our work with awake behaving macaques requires using the fewest macaques necessary. A sample size of two to three is common in behavioral neuroscience experiments with macaques provided that results are robust within each individual and that the effects generalize beyond one animal, as they do (see manuscript). Training macaques for awake MRI scanning requires a substantial time investment, and the data that was combined for each of these datasets in each of the three animals are individually robust and sufficiently powered (5 scanning sessions, ~75min of dMRI data that was collected and concatenated). The results are also consistent across the three animals, and the same sample size in chimpanzees and humans allowed cross-species comparisons that were stronger than individual differences even in these samples. Thus there was little ethical justification to train and test additional monkeys. The manuscript is also informed by one ultra-high resolution post mortem macaque dataset that had been shared as a resource previously. To allow direct comparisons across the species, 3 chimpanzee and 3 human datasets were randomly selected from available resources (http://www.chimpanzeebrain.org, group S500 of the Human Connectome Project). A random number generator was used to select the 3 datasets for each of these species, limited to male individuals only, to match to the three male awake macaque datasets available. Only these were analyzed. Moreover, the functional imaging data (tonotopic) probabilistic maps in macaques are based on the majority overlap of 10 macaques' fMRI localizer data that were obtained over the course of the last 10 years. The chimpanzee auditory ROIs were based on tonotopic mapping conducted under anesthesia by Bailey et al., 1943. The human tonotopic maps were based on tonotopic and myelin maps in over 50 individuals, as noted in the paper. Please note that the seminal Rilling et al., 2008 paper's hypothesis was reported data in 3 chimpanzee and 2 macaque post-mortem dMRI datasets.
Data exclusions	No data were excluded from any statistical analyses. In one macaque we observed low SNR in one hemisphere that may be implant related and could not be avoided, affecting the dorsal pathway signal in the left hemisphere. Therefore, to avoid suggesting spurious right lateralization effects these data were omitted only from the illustrative heat map summary (Fig. 1D) but are included in the other analyses and the interpretation of the results is based on all of the data.
Replication	In primate neuroscience it is common to assess effects in individual animals, rather than at a group level, with additional animals acting as a replication of these findings. There were also internal checks via patterns expected in the results from each of the species (ventral pathway being dominant and symmetric in macaques and chimps; consistency with an independent ultra-high resolution post mortem dataset; left lateralized human arcuate fasciculus). Moreover, in all species, the analyses and results produced highly similar results in all individuals and data available (see Figure 1 and 2).
Randomization	Macaque datasets were acquired as noted. Human and chimpanzee datasets were randomly sampled from the noted resources to match the macaque samples.
Blinding	The analyses were conducted automatically with anatomically or functionally predefined regions in the analyses pipelines. It was not possible to blind the investigators to the species of the animals while analyzing the dMRI datasets (the brains of the species are obviously different) but the results replicated expected effects in each species and had several internal controls.

Reporting for specific materials, systems and methods

We require information from authors about some types of materials, experimental systems and methods used in many studies. Here, indicate whether each material, system or method listed is relevant to your study. If you are not sure if a list item applies to your research, read the appropriate section before selecting a response.

Materials & experimental systems

n/a	Involved in the study
☒	☐ Antibodies
☒	☐ Eukaryotic cell lines
☒	☐ Palaeontology
☐	☒ Animals and other organisms
☐	☒ Human research participants
☒	☐ Clinical data

Methods

n/a	Involved in the study
☒	☐ ChIP-seq
☒	☐ Flow cytometry
☐	☒ MRI-based neuroimaging

Animals and other organisms

Policy information about studies involving animals; ARRIVE guidelines recommended for reporting animal research

Laboratory animals	Diffusion-weighted MRI scans in the awake macaques were acquired in three adult male rhesus macaques (macaca mulatta) weighing respectively 10kg, 16kg and 12kg and aged 10, 13 and 7. The other datasets were acquired and reported in previous publications (only analysis of the data in this report). The chimpanzee datasets are from an available resource (http://www.chimpanzeebrain.org).
Wild animals	The study did not involve wild animals
Field-collected samples	The study did not involve any field collected samples
Ethics oversight	All procedures conducted with the macaques were approved by the Animal Welfare and Ethical Review Body (AWERB) and the UK Home Office (project license: PA2C18B73) and are in full compliance with both the UK Animal Scientific Procedures Act (ASPA) and the European Directive (2010/63/EU) on the care and use of animals in research. We support the principles of the consortium on Animal Research Reporting of In Vivo Experiments (ARRIVE). The procedures were strictly regulated and all staff working with the animals held Home Office approved personal licenses and had received the accredited training and certification, as well as supervision and oversight of their work.

Note that full information on the approval of the study protocol must also be provided in the manuscript.

Human research participants

Policy information about studies involving human research participants

Population characteristics	The human datasets are from available resources (group S500 of the Human Connectome Project: http://www.humanconnectomeproject.org/).
Recruitment	As specified by the Human Connectome project: institutional oversight statements online.
Ethics oversight	Human Connectome institutional oversight.

Note that full information on the approval of the study protocol must also be provided in the manuscript.

Magnetic resonance imaging

Experimental design

Design type	dMRI data acquisition as described above and in the online methods
Design specifications	multiple scanning sets in each animal
Behavioral performance measures	fixation task to ensure the animal was awake and to allow it to obtain rewards for participating during the scan

Acquisition

Imaging type(s)	diffusion imaging
Field strength	4.7 Tesla
Sequence & imaging parameters	Spin Echo diffusion weighted EPI, matrix 88x88, 56slices, isotropic 1mm voxel. 4 saturation slices used to suppress signal for temporal muscles, eyes, mouth and back of the neck. TR=14s, TE=56ms, parrallel imaging acceleration factor=2 4 channels receive coil array (see paper for further details).
Area of acquisition	whole brain

Diffusion MRI ☒ Used ☐ Not used

Parameters: 60 directions, B=800s/mm2 , multi-shell

Preprocessing

Preprocessing software: FSL diffusion toolbox

Normalization: normalization was conducted as part of the diffusion parameters calculation (FSL BEDPOSTX)

Normalization template: not used, analyses conducted in the animal's native space for greater precision. ROIs were registered to the animals native space from the atlases or ROIs registered on a standard template brain (see paper).

Noise and artifact removal: None

Volume censoring: None

Statistical modeling & inference

Model type and settings: Repeated Measures ANOVA model was implemented in SPSS with all the dMRI data for the three-way cross species comparison. Model assumptions were met or corrected results values reported.

Effect(s) tested: The model contained the following factors: Within subjects factors of Pathway (dorsal, ventral), Hemisphere (left, right); Between subjects factor of Species (macaque, chimpanzee, human). All main effects and interactions are reported.

Specify type of analysis: ☐ Whole brain ☒ ROI-based ☐ Both

Anatomical location(s): ROIs used functionally defined tonotopic maps obtained in different individuals (macaques, chimps and humans). Accepted anatomical ROIs from atlases were also used in analyses, registered to each subjects native space.

Statistic type for inference (See Eklund et al. 2016): Multi-factorial results as F test, with reported or corrected degrees of freedom and actual p-values reported.

Correction: Variance assumptions met

Models & analysis

n/a	Involved in the study
☒	☐ Functional and/or effective connectivity
☒	☐ Graph analysis
☒	☐ Multivariate modeling or predictive analysis